

## Effect of Pt incorporation into $\text{Ni}/\text{ZrO}_2\text{--SO}_4^{2-}/\text{Al}_2\text{O}_3$ catalyst for *n*-butane isomerization

M. Pérez-Luna<sup>a,b,\*</sup>, A. Cosultchi<sup>a</sup>, J. A. Toledo-Antonio<sup>a</sup>, C. Angeles-Chavez<sup>a</sup>, and E. M. Arce-Estrada<sup>b</sup>

<sup>a</sup>Instituto Mexicano del Petroleo, Eje Central "L. Cardenas" No. 152, 07730 México D.F.

<sup>b</sup>Department of Metallurgical Engineering-ESIQIE, Instituto Politécnico Nacional, UASLP, Zacatenco, 07738 Mexico D.F., Mexico

Received 23 July 2005; accepted 18 November 2005

Three  $\text{Ni}/\text{ZrO}_2\text{--SO}_4^{2-}/\text{Al}_2\text{O}_3$  catalysts with different concentrations of platinum (0.2, 0.3 and 0.4 wt%) were prepared and tested for *n*-butane isomerization reaction at 338 K, in absence and in presence of hydrogen. The results shown that, at low temperature, platinum contributes to the olefin or butyl ion formation and the reaction follows a bimolecular pathway. However, when the reaction occurs in the presence of hydrogen, the formation of butyl ions is inhibited. The main feature of platinum addition is the stabilization of the catalytic activity, which is indicated by the slow deactivation constants compared to that of the unpromoted catalyst.

**KEY WORDS:** *n*-butane isomerization; Pt catalyst;  $\text{Ni}/\text{ZrO}_2\text{--SO}_4^{2-}/\text{Al}_2\text{O}_3$  catalyst.

### 1. Introduction

Isomerization of straight-chain paraffins such as *n*-butane to branched hydrocarbons is a good alternative to improve the motor fuel quality. Sulfated zirconia materials show remarkable catalytic activity for such reaction, although, the isomerization activity declines rapidly [1]. The high catalytic activity was attributed to the superacidity of this material [2], although, other authors claimed that the acidity of this material is weaker than that of alumina [3]. Moreover, the time of life of such material is still short; they deactivate rapidly. Such deactivation occurs not only by coke deposition but also by reduction of oxidation state of sulfur in the surface complex [4,5].

Incorporation of metallic species such as Pt, Ni, Sn, W or Fe to sulfate zirconia catalyst allows the improvement of the surface acidic properties rather than with the amorphous silica–alumina materials [6]. Metals which usually have hydrogenation/dehydrogenation functions may be used to stabilize the activity of anion-modified zirconia catalysts. Especially, adding platinum group metals improved their long-term stability [7–9]. The stability of a  $\text{SO}_4^{2-}/\text{ZrO}_2$  catalyst with Pt was attributed to coke inhibition by the stream of gas containing hydrogen at high pressure [7,10].

The effect of Pt to the generation of activated hydrogen able to inhibit the coke formation is referred as 'hydrogen spillover' and implies dissociation of molecular hydrogen followed by the diffusion of  $\text{H}^+$

onto the support; thus, the hydrogen ion is supposed to act as a protonic site on the catalyst surface [9,10]. Although most authors also indicate that platinum works as a hydrogen transfer agent by regenerating the acid sites after the organic cations were desorbed from the catalyst surface [7,9,10,12], some other studies indicate that at high pressure of hydrogen the activity of a sulfated zirconia catalyst is suppressed [13]. Apparently, the main aspect of Pt incorporation is related to its influence on the zirconia crystal phase and not to its metallic properties [14].

Consequently, one of the beneficial effects of Pt addition to a superacid catalyst is the improvement of the catalysts stability and selectivity. Nonetheless, the reaction mechanism is still considered monofunctional, since no increase of the catalysts activity was observed for the *n*-butane isomerization in the presence of the metallic phase [5]. Moreover, the amounts of Lewis and Brønsted acid sites determined by infrared spectroscopy are apparently independent of the Pt loading [8]. Thus, the metallic properties of platinum are suppressed due to the strong interaction with the support [11], which indicated that alumina is a more convenient support for Pt, as it improves both catalytic activity and stability of the catalyst.

In addition, Ni–Pt bimetallic catalysts on acidic supports, used for hydroisomerization, have shown enhanced isomerization activity than Pt only containing catalyst. Apparently, Pt plays an important role in suppression of the oxidation of Ni surface and retains the active NiO surface, while adding Ni up to a threshold value may sustain the catalyst activity compared to Ni free of Pt catalysts [15].

\*To whom correspondence should be addressed.

E-mail: mperezl@imp.mx

In this work, instead of preparing separately the sulfated zirconia and the Pt impregnation on alumina [11], the platinum is incorporated to the alumina-promoted nickel sulfated zirconia catalyst. This method was proposed by Manoli [16] which obtained a catalyst with improved activity if compared to the regular preparation via introducing platinum after catalyst calcination.

The activity and selectivity of the catalysts at three platinum concentrations (0.2, 0.3 and 0.4 wt%) were evaluated for *n*-butane isomerization reaction with and without H<sub>2</sub>. All the results are compared with the Ni/ZrO<sub>2</sub>-SO<sub>4</sub><sup>=</sup>/Al<sub>2</sub>O<sub>3</sub> catalyst non-promoted with platinum.

## 2. Experimental

### 2.1. Synthesis of materials

The Zr(OH)<sub>4</sub> was prepared by precipitation of a 20 wt% [ZrO(NO<sub>3</sub>)<sub>2</sub> Aldrich 99.9%] solution with a 28 wt% NH<sub>4</sub>OH (J.T. Baker) solution, added drop by drop until a pH of 8–9 is reached [2]. The precipitate cake was washed and filtered repeatedly with deionized water until a neutral pH is obtained. Thereafter the clean filtrated cake was dried overnight, then, it was mixed with a 2N H<sub>2</sub>SO<sub>4</sub> solution containing Nickel nitrate (Ni(NO<sub>3</sub>)<sub>2</sub>·6H<sub>2</sub>O). The alumina-promoted catalyst (Ni/ZrO<sub>2</sub>-SO<sub>4</sub><sup>=</sup>/Al<sub>2</sub>O<sub>3</sub>) was prepared by wet method, adding boehmite (Catapal, Vista) to the NiZrS catalyst. Parts of this catalysts were impregnated with a PtCl<sub>4</sub> (Aldrich al 99%) solution of different concentrations, made with deionized water and, using the incipient wetness impregnation method. Based on our previous work, the optimum amount of alumina added was 17.5 wt%, without weakening the catalytic activity of Ni/ZrO<sub>2</sub>-SO<sub>4</sub> catalyst as shown elsewhere [17].

The three samples obtained after platinum impregnation were dried for 12 h at 383 K. All powder samples were manually extruded to obtain 1/8" cylindrical forms with a peptizer (1/32 diluted HNO<sub>3</sub>) and, annealed at 948 K for 1 h in flowing air. The samples were labeled NiZrSAI-Ptx, where Ni means nickel, Zr zirconia, S sulfate, Al alumina, Pt is platinum and, *x* is the percent of Pt. Table 1 shows the chemical composition of the prepared catalysts.

### 2.2. Characterization techniques

The chemical composition was determined by Atomic Absorption Spectroscopy in a Perkin Elmer S-2380 apparatus; the amount of sulfur was determined by combustion in a LECO SC-44 apparatus. Specific surface area measurements were carried out in a Micromeritics Digisorb 2600 apparatus according to ASTM-D-3663. X-ray diffraction patterns of powdered samples were recorded at room temperature with CuK<sub>α</sub> radiation Siemens D500 diffractometer having theta–theta configuration and a graphite secondary-beam monochromator. The Diffraction pattern was recorded in the 2θ range between 10 and 70°. The Rietveld technique with FULLPROF-V3.5d codes was used to refine the crystallite size, and the relative content of crystalline phases of ZrO<sub>2</sub>.

The total acidity was measured by NH<sub>3</sub> titration in an Altamira AMI 2000 equipped with a thermal conductivity detector (TCD). Two-hundred mg of sample was pretreated under flowing N<sub>2</sub> at 773 K for 4 h. Then, the sample was cooled down to 423 K. Calibrated pulses of NH<sub>3</sub> were injected through a 6 port on-line valve until saturation of the sample was reached. The amount of NH<sub>3</sub> adsorbed by the sample was calculated from the difference between total NH<sub>3</sub> injected and the amount of NH<sub>3</sub> calculated from the TCD signals.

The nature of the surface acidity was tested by pyridine vapors (py) adsorption/desorption at two temperatures: 323 and 573 K, respectively [13]. The sample was evacuated up to 10<sup>−1</sup> Pa; maintained under nitrogen flow saturated with pyridine (2.14 mL h<sup>−1</sup>) for 15 min. After that, the sample was outgassed at 10<sup>−1</sup> Pa for 1 h at room temperature and, the infrared spectra were registered at two temperatures: 323 and 573 K after evacuation of the adsorbed pyridine. The characteristic bands of pyridine protonated by Brönsted acid sites appear at 1545 cm<sup>−1</sup> (at 323 K) and 1640 cm<sup>−1</sup> (at 573 K) while the bands of pyridine coordinated to Lewis acid sites appear at 1455 cm<sup>−1</sup> (at 323 K) and 1610 cm<sup>−1</sup> (at 323 K). From the intensity of such bands it is possible to calculate the Brönsted and Lewis acid sites of the catalyst [18].

Transmission electron microscopy, TEM, was performed in a Tecnai F30 S-twin transmission electron microscope with accelerating voltage of 300 kV and 0.2 nm of resolution. Electron microscopy specimens

Table 1  
Chemical composition of the catalyst samples

Catalyst	Chemical composition wt%				
	ZrO <sub>2</sub>	NiO	SO <sub>4</sub>	Al <sub>2</sub> O <sub>3</sub>	Pt <sub>2</sub> O
NiZrSAI	78.3	0.8	3.3	17.5	0.00
NiZrSAI-Pt 0.2	78.1	0.8	3.3	17.5	0.19
NiZrSAI-Pt 0.3	78.1	0.8	3.3	17.5	0.29
NiZrSAI-Pt 0.4	78.1	0.8	3.3	17.4	0.39

were prepared by depositing the particles of the samples to be investigated onto holey carbon coated 3-mm Cu grids

### 2.3. Catalytic activity evaluation

The catalytic acidity of solids was evaluated using *n*-butane isomerization reaction. The reaction was carried out in a stainless-steel fixed bed microreactor (7 mm of diameter, 150 mm of length) using 0.5 g powdered sample previously treated under flow air (30 cm<sup>3</sup>/min) at 773 K for 1 h.

The operation conditions for the catalytic evaluation without H<sub>2</sub> were as follows: the *n*-butane (Matheson C.P.) flow was 2.5 mL/min, the temperature was fixed at 338 K and, the pressure at 2.5 kg/cm<sup>2</sup>, which are below the critical conditions for the *n*-butane isomerization [19]. In the second set of experiments, the operation conditions were similar and the inlet flow of gases was maintained at the same pressure but with a H<sub>2</sub>/*n*-butane ratio of 0.05.

The reaction products were analyzed on-line in a Hewlett-Packard 5890 Gas Chromatograph equipped with a 3 m × 1/8" packed column (Porasil C) and, TCD detector.

## 3. Results

### 3.1. Textural, structural and, acid properties of the catalysts samples

Table 2 shows the textural properties of the catalysts. The increase of the specific area is related to the amount of Pt added to the catalyst. Hence, for the Pt-promoted catalysts, the specific area is about 15% higher than that of the unpromoted catalyst. The same occurs with the porous volume, which showed a gradual increase with the Pt content, the increase is 17.4%. Considering the experimental error, the mean pore diameter remained around 50.6 Å and with a standard deviation of 2.16 Å, independently on the amount of Pt loaded.

Figure 1 shows the X-ray diffraction patterns of the studied catalysts after their calcinations at 948 K. The peak at 2θ = 40° corresponds to platinum as indicated elsewhere [5] and its intensity increases according to the amount of metal added to the catalyst. The diffraction peaks at 2θ = 45.5° and 66° correspond to γ-alumina

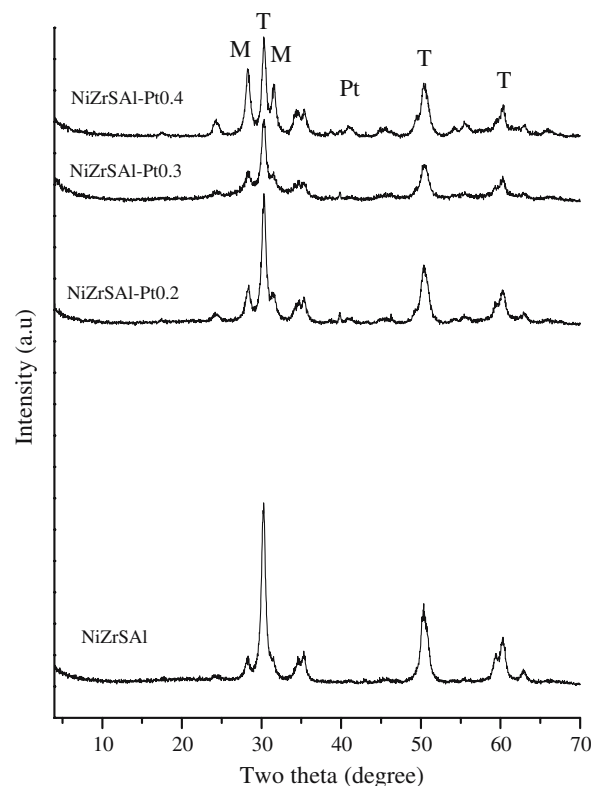


Figure 1. X-ray diffraction patterns of the catalysts evaluated in this study. (T corresponds to ZrO<sub>2</sub> tetragonal phase, M to ZrO<sub>2</sub> monoclinic phase and Pt to platinum).

and, they are weak as an indication of its amorphous structure. Table 3 shows the amounts of tetragonal and monoclinic zirconia phases determined by Rietveld analysis of the diffractograms.

As more platinum was added to the catalyst, the amount of the zirconia tetragonal phase decreased following a linear decay:

$$y = -6.214x + 78.115 \quad (1)$$

where *y* is the wt% of zirconia tetragonal phase and *x* is the wt% of platinum.

The amount of platinum added to the catalyst composition contributes to increase the crystal size of the tetragonal phase; the lowest crystal size value, 148.4 Å, was observed in absence of platinum. When platinum was added to the catalyst, the tetragonal ZrO<sub>2</sub> crystallite size stabilizes to a mean value of approximately 248 Å independently of the platinum amount. Consequently, the monoclinic phase concentration increased and also its crystallite size.

Figure 2a shows the HRTEM micrograph of the NiZrSAI-Pt 0.3 catalyst and the FFT pattern in the insert of the upper part of the image. This sample contains mostly zirconium particles, identified by the as monoclinic phase from the spots in (111) and (002) planes. In addition, some small and dark nanoparticles, marked by arrows, can be observed as highly dispersed

Table 2  
Textural properties of the catalyst samples

Catalyst	Specific area (m <sup>2</sup> /g)	Pore volume (cm <sup>3</sup> /g)	Mean pore diam. (Å)
NiZrSAI	116.5	0.133	46.8
NiZrSAI-Pt 0.2	132.4	0.148	51.27
NiZrSAI-Pt 0.3	132.6	0.159	52.27
NiZrSAI-Pt 0.4	137.8	0.161	48.13

Table 3  
ZrO<sub>2</sub> crystal size, the amounts of tetragonal and, monoclinic phases of the catalysts

Catalyst	Zirconia crystallite size, Å		ZrO <sub>2</sub> phases, wt%	
	Tetragonal	Monoclinic	Tetragonal	Monoclinic
NiZrSAI	148.4	137.0	71.6	8.3
NiZrSAI-Pt 0.2	252.2	218.20	66.15	11.25
NiZrSAI-Pt 0.3	235.6	223.50	59.45	18.18
NiZrSAI-Pt 0.4	255.4	248.0	53.12	24.34

on the catalyst particles. After Fourier filtering of the HRTEM image, figure 2b shows the platinum nanoparticles are clearly observed as black points dispersed on the amorphous alumina support, some of them are marked by arrow. The sizes of these nanoparticles have a range between 1 and 2 nm.

Table 4 shows the experimental data of the acid site density of the catalyst samples measured by ammonia temperature programmed desorption TPD-NH<sub>3</sub>. As observed in table 4, the surface area of the catalyst increases, from 116.5 m<sup>2</sup>/g, in the catalyst without platinum, to a mean value of 134 m<sup>2</sup>/g when Pt is loaded. The impregnation of catalyst with platinum acidic solution could have contributed to peptize the alumina and therefore, favored the increment of the surface area of about 15.25%.

It is also well known that when platinum is added to a catalyst, its acidity is not affected [16]. However, as table 4 shows, the density of the acidic sites diminishes from 11.6 mmol NH<sub>3</sub>/m<sup>2</sup> for the NiZrSAI to a mean value of 6.6 mmol NH<sub>3</sub>/m<sup>2</sup> for the Pt promoted catalysts.

Table 5 shows Brönsted and Lewis acid sites measured as the adsorbed pyridine, in mol of Py/g of catalyst. After the samples were outgassed at 323 K, an increase in both Brönsted and Lewis acid sites was observed; the B/L ratio is 0.22 for NiZrSAI without platinum, but the same value is observed when 0.2 and 0.3 wt% of platinum is added to the catalyst. When 0.4 wt% of platinum is added to the catalyst, there is an increase in the density of the Brönsted sites increasing the B/L ratio to 0.456. This value is not an odd value, as B/L ratios of 1 or 0.5 were previously reported for *n*-butane isomerization reaction [20,21].

Outgassing at 573 K has a different effect on catalyst acidic properties, as the amount of pyridine adsorbed on the sample is reduced. This confirms that the acidity strength of these materials is weak, as they loose most of their acid sites at higher temperatures such as 573 K. This wakening could also be attributed to the peptizing of alumina.

### 3.2. Activity of the catalysts tested in *n*-butane isomerization reaction

Figure 3 shows the conversion of *n*-butane during the isomerization reaction in the absence of hydrogen, at

different time on stream and using each of the tested catalysts. The presence of platinum in the catalysts contributes to stabilize the *n*-butane conversion for a long time on stream. In fact, while in absence of platinum the catalyst completely deactivate at 10 h, the platinum containing samples maintain conversion as high as 20 mol%. Then, the main effect of platinum is to inhibit the deactivation.

The deactivation constant ( $K_d$ ) is estimated from the deactivation slope of the Pt-containing catalysts which follows the equation:

$$\ln(1 - X_a)/X_a = K_d * t + (1 - X_{ao})/X_{ao} \quad (2)$$

where  $X_a$  is the conversion at any time on stream,  $X_{ao}$  is the conversion at time near to zero,  $K_d$  is the deactivation constant and,  $t$  is the time on stream.

Table 6 shows the results of the conversion data fitting. The value of the deactivation constant ( $K_d$ ) for the unpromoted catalyst was at least five times higher than that for the Pt-promoted catalysts at any concentration. The experimental data show a very good linear fit with regression coefficients ( $R^2$ ) higher than 0.9.

Figure 4, shows the deactivation linear plots for catalyst without platinum and for the sample containing 0.4 wt% of platinum. As observed in this figure, the deactivation is faster for the unpromoted catalyst, than for the platinum promoted catalyst.

The catalytic activity results in figure 4 and table 2 also show that when platinum is incorporated in a superacid catalyst, such as NiZrSAI, it contributes to slow down the catalyst deactivation, which confirms the Garin findings [7]. Thus, the material containing platinum still works after 24 h on stream, while the material without platinum loses its activity after 9 h.

Table 7 shows the composition of the outlet gas for each catalyst and for 10 h on stream. The other reaction products consist mainly of propane, methane, ethylene and traces of isopentane.

Table 8 shows the results of the conversion of *n*-butane during the isomerization reaction obtained in the presence of H<sub>2</sub>, the conversion levels were lower than those obtained when the reaction was developed without hydrogen.

When metals are incorporated to a sulfated zirconia catalyst, it is well-known that the selectivity towards isobutane is improved [22]. The selectivity interval is

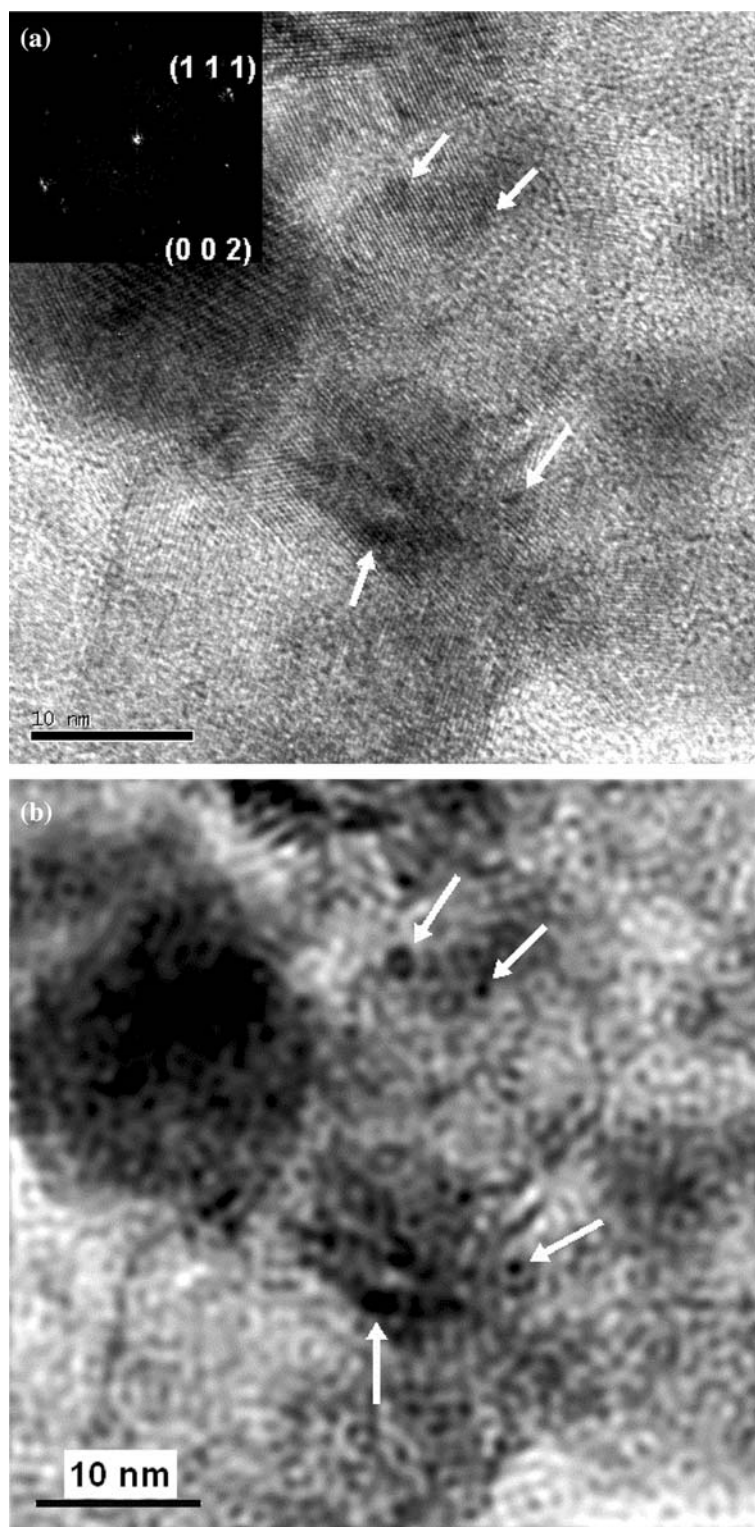


Figure 2. (a) HR-TEM micrographs of 0.3%Pt-NiZrSAI sample. Inset FFT pattern showing zirconia monoclinic phase. (b) Filtered image of the corresponding HR-TEM image highlighting platinum nanoparticles.

also improved, 94–98 mol% for 24 h on stream, while in the absence of platinum, the selectivity interval is lower, 91.5–97 mol% and, the catalyst only works 9 h on stream.

#### 4. Discussion

The most important function of platinum in a catalyst refers to the generation of activated hydrogen, able

Table 4  
Ammonia temperature programmed desorption results

Catalyst	Surface area, $\text{m}^2 \text{g}^{-1}$	TPD acidity $\text{mmol NH}_3/\text{g}$	Acid sites density $\text{mmol NH}_3 \text{m}^{-2}$
NiZrSAI	116.5	1350.6	11.59
NiZrSAI-Pt 0.2	132.4	879	6.63
NiZrSAI-Pt 0.3	132.6	905	6.83
NiZrSAI-Pt 0.4	137.8	887	6.43

to inhibit the coke formation [11]. However, the results of the experiments presented in this work indicated that the addition of platinum modifies, in a positive way, the textural and the acid properties of the NiZrSAI catalyst.

First, the specific area and the porous volume increased when platinum is added to the catalyst. Such increase follows the rising branch of a second-degree polynomial path, and indicates that the maximum values of these parameters are reached for 0.4 wt% of platinum. In the case of a zirconia catalyst, the smaller the crystal size of this zirconia active phase the better should be its catalytic activity [23]. However, in the present experiments, platinum apparently contributes to increase the dimensions of zirconia tetragonal crystallites without any detrimental effect on their catalytic activity. Moreover, platinum addition decrease the concentration of the tetragonal phase, but the catalytic activity was maintained. The effect, of the platinum on the texture, structure can be explained as the platinum was introduced since the synthesis. The samples were calcined within platinum already impregnated, contrary to other procedures where platinum is normally incorporated after the sulfated zirconia catalyst has been calcinated. The HR-TEM observations show platinum nanoparticles of 1–2 nm of diameter and no massive platinum aggregates. Moreover, these particles are randomly, and preferentially dispersed on alumina surface instead on zirconia crystals, which is due to the fact that alumina surface is more negatively charged than zirconia. Consequently, the sintering of platinum nanoparticles is inhibited.

In addition, the acidity of the material, measured by  $\text{NH}_3$  titration, diminished when platinum is added following the descending branch of a second-degree polynomial path, until a plateau is reached for 0.4 wt% of platinum. On the contrary, the amount of Brönsted and

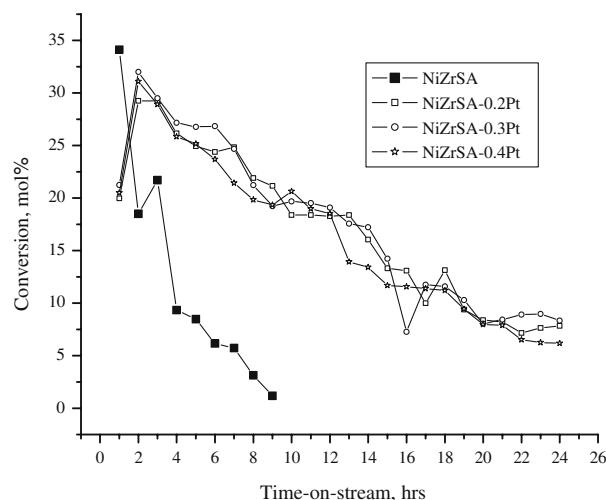


Figure 3. Conversion of *n*-butane versus time on stream for each catalyst.

Lewis sites, measured as the adsorbed pyridine, in mol of Py/g of catalyst, increases in the presence of platinum, as table 5 shown. It is well known that, both, Brönsted and Lewis acidic sites can form on the surface of the catalyst and the nature and, the strength of these sites depend on parameters such as: concentration of sulfates, adsorption of water, zirconia active phase crystallite sizes [18].

The surface properties of a superacid catalyst promoted by platinum and alumina are supposed to be modified only if hydrogen is used in the isomerization reaction [8–10]. The hydrogen effect on this reaction was controversial since the beginning. However, most studies on bifunctional catalysts promoted with Pt [24–27] indicated that hydrogen is an important ingredient in the alkane isomerization. Recent studies indicated that a series of factors such as: the type of metal promoter presents in the SZ catalyst, the purity of the alkane feed and, the reaction temperature are affecting the results of the isomerization reaction. Most studies agreed that when Ni or Pt are the promoters of the SZ catalysts, hydrogen increases the *n*-butane conversion only if the reaction temperature is higher than 523 K and the *n*-C<sub>4</sub>/H<sub>2</sub> ratio is 0.5 [28]. The reaction, however, is inhibited and the catalyst deactivates at temperatures below 473 K when H<sub>2</sub> or He are used as diluents. Thus, it is

Table 5  
Brönsted and Lewis acid sites measured as the adsorbed pyridine, mol of Py/g

Catalyst	At $T = 323 \text{ K}$				At $T = 573 \text{ K}$			
	Brönsted	Lewis	B/L ratio	Total mol py/g	Brönsted	Lewis	B/L ratio	Total mol py/g
NiZrSAI	32	144	0.222	176	0	39	0	39
NiZrSAI-Pt 0.2	32	159	0.201	191	15	38	0.394	53
NiZrSAI-Pt 0.3	47	215	0.218	262	26	99	0.262	125
NiZrSAI-Pt 0.4	85	186	0.456	271	0	0	0	0

Table 6

The deactivation constants for *n*-butane isomerization reaction in absence of H<sub>2</sub>

Catalyst	$K_d$ (deactivation constant), (h <sup>-1</sup> )	$X_{ao}$ (starting conversion)	$R^2$ (correlation coefficient)
NiZrSAI	0.4062	74.19	0.94
NiZrSAI-Pt 0.2	0.0817	61.69	0.97
NiZrSAI-Pt 0.3	0.0790	62.15	0.97
NiZrSAI-Pt 0.4	0.0875	61.39	0.98

worth to note that the catalysts prepared and evaluated in this work contain both metals Ni and Pt but the results shown that the isomerization reaction is sensitive to hydrogen. The activity of the Pt-promoted catalysts evaluated in the present work, in the presence of hydrogen at 338 K; 2.5 kg/cm<sup>2</sup> of pressure and using a H<sub>2</sub>/C<sub>4</sub> ratio of 0.05, shown a decay of the catalysts

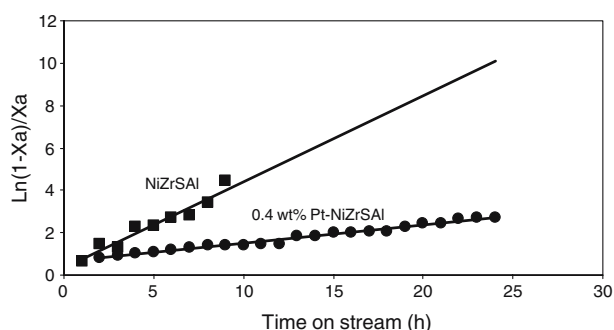


Figure 4. Logarithm plots from linearization of the conversion data of the NiZrSAI and 0.4 wt% Pt-NiZrSAI samples.

Table 8

Conversions of *n*-butane in presence of H<sub>2</sub> and up to 3 h on-stream

Catalyst	1 h	2 h	3 h
NiZrSAI-Pt-0.2	2.10	1.40	1.40
NiZrSAI-Pt-0.3	7.90	10.00	4.20
NiZrSAI-Pt-0.4	11.40	1.10	0.00

activity. On the contrary, in the absence of hydrogen, the catalysts displayed an important increase in its activity and its lifetime.

The *n*-butane isomerization may occur through any of the two possible mechanisms: (a) the monomolecular pathway, which consists in an intramolecular rearrangement and, (b) the bimolecular pathway, accompanied by intermolecular rearrangement. Nonetheless, contradiction on which is the adequate mechanism appears since the catalyst was formulated [3,7]. In recent studies on the isomerization mechanism [24–26,29,30], the authors indicated that, in the presence of hydrogen in the feed, the rate of butane isomerization decreases and the reaction pathway is apparently monomolecular. At high hydrogen pressure the reaction mechanism shifts towards a bimolecular pathway and hydrogenolysis. Apparently, other promotional effect of platinum is the olefin formation, as the *in-situ* reactive intermediate of the surface chain isomerization reaction, leading the reaction by a bimolecular pathway [30]. Moreover, platinum promotes the olefin formation leading the reaction by a bimolecular pathway.

Thus, a positive evidence of a bifunctional mechanism should be an important increase of the catalytic

Table 7

Composition of the outlet gas, wt%

Catalyst	Compound	Time on stream, hours									
		1	2	3	4	5	6	7	8	9	10
NiZrSAI	C1–C2	0	0	0	0	0	0	0	0	0	0
	C3	0.538	0.39	0.305	0.195	0.291	0.075	0.115	0.055	0.03	0.017
	<i>i</i> -C4	32.779	17.65	20.865	8.92	8.041	5.972	5.42	2.99	1.08	0.314
	<i>n</i> -C4	65.890	81.51	78.29	90.65	91.53	93.83	94.27	96.86	98.82	99.556
	C5+	0.793	0.45	0.54	0.235	0.138	0.123	0.195	0.095	0.07	0.113
NiZrSAI-Pt 0.2	C1–C2	0	0	0	0	0	0	0	0	0	0
	C3	0.45	0.395	0.485	0.395	0.318	0.249	0.279	0.259	0.318	0.364
	<i>i</i> -C4	19.642	30.187	28.041	24.647	24.45	22.84	20.872	18.873	18.546	19.962
	<i>n</i> -C4	79.49	68.87	71.1	74.15	74.83	76.32	78.56	80.17	80.66	79.37
	C5+	0.418	0.548	0.374	0.808	0.402	0.591	0.289	0.698	0.476	0.304
NiZrSAI-Pt 0.3	C1–C2	0	0.015	0.026	0	0	0.016	0	0	0	0
	C3	0.277	0.538	0.435	0.369	0.533	0.476	0.37	0.43	0.391	0.35
	<i>i</i> -C4	20.4	30.664	28.425	26.143	25.603	25.84	23.831	21.237	18.419	18.945
	<i>n</i> -C4	78.75	67.99	70.49	72.85	73.23	73.15	75.31	77.903	80.77	80.31
	C5+	0.573	0.793	0.624	0.638	0.634	0.518	0.489	0.43	0.42	0.395
NiZrSAI-Pt 0.4	C1–C2	0	0	0	0	0	0	0	0	0	0
	C3	0.33	0.223	0.238	0.314	0.247	0.237	0.271	0.301	0.159	0.236
	<i>i</i> -C4	19.247	27.636	27.6	25.483	24.33	23.826	24.323	21.127	20.742	17.849
	<i>n</i> -C4	80.02	71.74	71.74	73.84	75.06	75.62	75.15	78.1	78.83	81.61
	C5+	0.403	0.401	0.422	0.363	0.363	0.317	0.256	0.472	0.269	0.305



activity when hydrogen is absent; whereas, hydrogen presence in the reaction media at the temperature of 338 K, inhibit the formation of olefins and the conversion level drops.

The results of the present work are in agreement with the previous findings [25], where it is indicated that in the absence of hydrogen, the bimolecular pathway is favored if the reaction occurs at low temperature, the catalyst has high density of acidic sites, there is a long contact time with the reactant and, the feed has low dilution.

Normally, the lifetime of commercial catalysts containing chlorinated alumina for *n*-butane isomerization is maintained or improved in the presence of hydrogen. Hydrogen reacts with the disproportionation products of the isomerization reaction and, in this way the poisoning with coke of the catalyst is avoided [11,31]. This means that the metallic properties of the catalyst contribute to hydrogenate the olefins inhibiting the bimolecular mechanism in presence hydrogen in the reaction media. In the absence of hydrogen, platinum contribute to the formation of butyl ion, which conduct the reaction towards bimolecular pathway and inhibit the catalyst deactivation. In this case, the location of platinum has been also on discussion over the years [11]. Considering that Pt particles were covered with  $\text{SO}_4^{2-}$  due to the strong interaction with the NiZrSAI support, a complete structural study of Pt/sulfated zirconia catalysts indicated that the platinum particles are 'embedded' into sulfated zirconia crystals and partially covered by the support [16,32]. This is supposed to be an evidence of a solid-state rearrangement and may also have occurred with nickel, the other metallic species of this catalyst. However, when alumina is introduced in the catalyst, the HR-TEM images provide a strong evidence of Pt random dispersion on alumina which also preserve them from sintering. As the results showed, the catalytic activity is higher in absence of hydrogen, which means that this catalyst is sensitive to the presence of hydrogen; this occurs because the hydrogen produced during the disproportionation reaction is sufficient to conserve the catalysts activity for longer time if compared to that of the same catalyst working in the absence of platinum.

## 5. Conclusions

In absence of hydrogen in the reaction media, the main advantage of platinum incorporation to the NiZrSAI catalyst is the stabilization of the catalytic activity for the *n*-butane isomerization which is indicated by the slow deactivation constant compared to that of the  $\text{Ni}/\text{ZrO}_2\text{-SO}_4^{2-}/\text{Al}_2\text{O}_3$  unpromoted catalyst. When hydrogen was absent in the reaction media, platinum-promoted catalyst contributes to the formation of butyl ions or olefins and the reaction follows a

bimolecular mechanism. On the contrary, when hydrogen is present in the steam and the reaction occurs at low temperature (338 K), the formation of butyl ion is inhibited and consequently, the reaction mechanism changes to a monomolecular pathway.

## References

- [1] M. Hino, S. Kobayashi and K. Arata, *J. Am. Chem.* 101 (1979) 6439.
- [2] K. Shimizu, N. Kounami, H. Wada, T. Shishido and H. Hattori, *Catal. Lett.* 54 (1998) 153.
- [3] V. Adeeva, G.D. Lei and W.M.H. Sachtler, *Catal. Lett.* 33 (1995) 135.
- [4] J.C. Yori, J.C. Luy and J.M. Parera, *Catal. Today* 5 (1989) 493.
- [5] J.C. Yori, J.C. Luy and J.M. Parera, *Appl. Catal.* 46 (1989) 103.
- [6] V.C.F. Holm and G.C. Bailey, US Patent 3 032 599 (1962).
- [7] F. Garin, D. Adriamasiro, A. Abdulsamad and J. Sommer, *J. Catal.* 131 (1991) 199.
- [8] K. Ebitani, J. Konishi and H. Hattori, *J. Catal.* 130 (1991) 257.
- [9] E. Iglesia, S.L. Soled and G.M. Kramer, *J. Catal.* 144 (1993) 238.
- [10] K. Ebitani, H. Konno, T. Tanaka and H. Hattori, *J. Catal.* 135 (1992) 60.
- [11] J.C. Yori, M.A. D'Amato, G. Costa and J.M. Parera, *J. Catal.* 153 (1995) 218.
- [12] R. Srinivasan, T.R. Watkins, C.R. Hubbard and B.H. Davis, *Chem. Mat.* 7 (1995) 725.
- [13] A. Corma, *Chem. Rev.* 95 (1995) 559.
- [14] J.A. Grau, J.C. Yori, C.R. Vera, F.C. Lovey, A.A. Condo and J.A. Parera, *Appl. Catal.* 265(2) (2004) 141.
- [15] Eswaramoorthi Iyyamperunal and Lingappan Nachiyappan, *Korean J. Chem. Eng.* 20(2) (2003) 207.
- [16] J.-M. Manoli, C. Potvin, M. Muhler, U. Wild, G. Resofszki, Th. Buchholtz and Z. Paál, *J. Catal.* 178 (1998) 338.
- [17] M. Pérez-Luna, A. Cosultchi, J.A. Toledo-Antonio and E.M. Arce-Estrada, *Catal. Lett.* 102(1–2) (2005) 33(6).
- [18] C. Morterra, G. Cerrato and V. Bolis, *Catal. Today* 17 (1993) 505.
- [19] B. Sander, M. Thelen and B. Kraushaar-Czarnetzki, *Ind. Eng. Chem. Res.* 40 (2001) 2767.
- [20] M.A. Coehlo, D.E. Resasco, E.C. Sikabwe and R.L. White, *Catal. Lett.* 32 (1995) 253.
- [21] P. Canton, R. Olindo, F. Pinna, G. Strukul, P. Riello, M. Meneghetti, G. Cerrato, C. Morterra and A. Benedetti, *Chem. Mat.* 13 (2001) 1634.
- [22] R. Ahmad, J. Melsheimer, F.C. Jentoft and R. Schlögl, *J. Catal.* 218 (2003) 365.
- [23] W. Stichert and F. Schüth, *Chem. Mater.* 10 (1998) 2020.
- [24] V. Nieminen, M. Kangas, T. Salmi and D.Yu. Murzin, *Ind. Eng. Chem. Res.* 44 (2003) 471.
- [25] T. Echizen, T. Suzuki, Y. Kamiya and T. Okuhara, *J. Mol. Catal. A: Chem.* 209 (2004) 145.
- [26] Y. Ono, *Catal. Today* 81 (2003) 3.
- [27] T. Suzuki and T. Okuhara, *Catal. Lett.* 72(1–2) (2001) 111.
- [28] W.E. Alvarez, H. Liu and D.E. Resasco, *Appl. Catal. A: Gen.* 162 (1997) 103.
- [29] K. Tomishige, A. Okabe and K. Fujimoto, *Appl. Catal. A: Gen.* 383 (2000) 194.
- [30] Z. Hong, K.B. Fogash, R.M. Watwe, B. Kim, B.I. Masquedá-Jiménez, M.A. Natal-Santiago, J.M. Hill and J.A. Dumesic, *J. Catal.* 178 (1998) 489.
- [31] J. Harver, J.H. Block and B. Delmon, *Pure Appl. Chem.* 67 (1995) 1257.
- [32] M. Guisnet, P. Andy, N.S. Gnep and C. Travers, *Ind. Ing. Chem. Res.* 37 (1998) 300.